The Chern-Simons diffusion rate in Improved Holographic QCD

Ioannis Iatrakis[α]
In collaboration with U. Gursoy, E. Kiritsis, F. Nitti, and A. O'Bannon.

[α] Physics & Astronomy Department, Stony Brook University

February 14, 2014

Outline

The chiral magnetic effect

- The Chiral magnetic effect is argued to take place when matter with net chirality is put in a background magnetic field, (Fukushima-Kharzeev -McLerran-Warringa).
- Right-handed particles move along the direction of their spin and left-handed particles in opposite direction than their spin. In case of strong magnetic field the spins of positively charged particles align in the direction of the field. The spin of negative charged particles is opposite.
- Therefore, net chirality creates an electric current parallel to the magnetic field.

The chiral magnetic effect

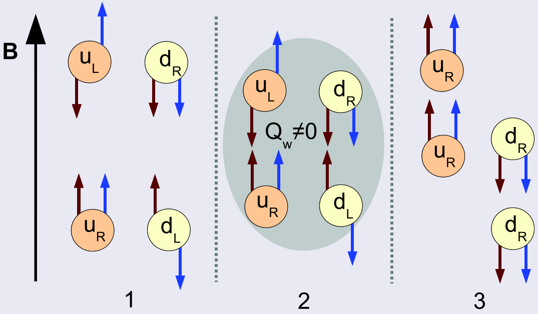

Figure : The red and blue arrows denote the momentum and spin, respectively. When a strong magnetic field, $\vec{B}$, is exerted in a medium of charges the positive charges align towards $\vec{B}$ and the negative opposite to $\vec{B}$. Moreover, right-handed particles move in the same direction with their spin and left-handed in the opposite, (1). When, the medium has net chirality, (2), separation of charges takes place, (3), (Kharzeev-McLerran-Warringa).

- Chern-Simons number, $N_{\rm CS}$, characterizes vacua of $SU(N_c)$ YM which cannot be connected with continuous gauge transformations

$$N_{\rm CS} \equiv \frac{1}{8\pi^2}\int d^3x\, \epsilon_{ijk}\, \mathbb{T}r\left[A_i\partial_j A_k - \frac{2ig}{3}A_iA_jA_k\right] , \tag{1}$$

where $i, j, k = 1, 2, 3$.

- The change in $N_{\rm CS}$ is

$$\Delta N_{\rm CS} = \int d^4x\, q(x^\mu) \; , \;\; q(x^\mu) \equiv \frac{1}{16\pi^2}\mathbb{T}r\,[F\wedge F] = \frac{1}{32\pi^2}\,\epsilon^{\mu\nu\rho\sigma}\mathbb{T}r F_{\mu\nu}F_{\rho\sigma} \, . \tag{2}$$

- Configurations with non-zero ΔN_{CS} lead to axial anomalies. Consider N_f massless fermions coupled to the YM. Then, the theory enjoys $U(N_f)_L \times U(N_f)_R$ global symmetry. The isospin singlet axial current is

$$j_5^\mu = \sum_{i=1}^{N_f} \overline{\psi}_i\gamma^\mu\gamma^5\psi_i \tag{3}$$

- This current is not conserved due to a quantum anomaly

$$\partial_\mu j_5^\mu = -\frac{N_f}{16\pi^2}\,\epsilon^{\mu\nu\rho\sigma}\mathbb{T}r F_{\mu\nu}F_{\rho\sigma}\,. \tag{4}$$

- Taking the expectation value of the above equation in some state and integrating over spacetime

$$\Delta N_5 = N_L - N_R|_{t=\infty} - (\,N_L - N_R|_{t=-\infty}) = 2N_f \Delta N_{CS}\,. \tag{5}$$

  Thus, changes in N_{CS} corresponds to a change in chirality of the medium.

- Consider now the transition amplitude, A, from a state $|\psi_1(t_1)\rangle$ to $|\psi_2(t_2)\rangle$ times the change in axial number

$$A\,\Delta N_5 = 2\int d^4x \langle\psi_2|q(x)|\psi_1\rangle \tag{6}$$

- Taking the square of the above equation, summing over all possible $|\psi_2(t_2)\rangle$ and using the completeness relation $\mathbb{I} = \sum |\psi_2\rangle\langle\psi_2|$

$$\langle(\Delta N_5)^2\rangle = 4 \int d^4x d^4y \langle\psi_1|q(x)q(y)|\psi_1\rangle \tag{7}$$

- The Chern-Simon diffusion rate, $\Gamma_{\rm CS}$, is the rate of change of $N_{\rm CS}$ per unit volume and is given by the Wightman two-point function of $q(x^\mu)$,

$$\Gamma_{\rm CS} \equiv \frac{\langle(\Delta N_{\rm CS})^2\rangle}{Vt} = \int d^4x \ \langle q(x^\mu)q(0)\rangle_W \ . \tag{8}$$

- In equilibrium states with finite temperature, $\Gamma_{\rm CS}$ is given by

$$\Gamma_{CS} = -\lim_{\omega\to 0} \frac{2T}{\omega} \,\mathrm{Im}\, G_R(\omega, \vec{k}=0)\,, \tag{9}$$

  where $G_R(\omega, \vec{k})$ is the Fourier tranformation of the retarted Green function of $q(x^\mu)$.
- The contribution of single instanton backgrounds to $\Gamma_{\rm CS}$ is exponentially suppressed.
- $\Gamma_{\rm CS}$ can be generated by thermal fluctuations in finite temperature states. Those excite shaleron configurations which produce non-zero $\Gamma_{\rm CS}$ upon decay.
- $\Gamma_{\rm CS}$ is zero in perturbation theory since $q(x)$ is a total derivative.
- Finite $\Gamma_{\rm CS}$ in QCD signals the creation of net chirality bubbles (domains of more left-handed than right-handed quarks or the opposite) because of the anomaly of the axial current.
- When those bubbles are in a background magnetic field, the chiral magnetic effect is created.

Improved Holographic QCD (IHQCD)

Fields & the dual operators

- Can we use gauge/gravity duality to calculate Γ_{CS}?
- IHQCD is an effective holographic model for 4d pure Yang-Mills. It's construction uses intuition from string theory and input from QCD (Gursoy-Kiritsis-Nitti).
- The bulk fields and their dual operators are

Bulk Fields		Dual Operator
Metric	$g_{\mu\nu}$	$\mathbb{T}r\left[F_{\mu\rho}F^{\rho}_{\nu} - \frac{\delta_{\mu\nu}}{4}F^2\right]$
Dilaton	ϕ	$\mathbb{T}r\left[F^2\right]$
Axion	α	$\mathbb{T}r\left[F \wedge F\right]$

Improved Holographic QCD (IHQCD)

The action

- The action of IHQCD is

$$S = M_p^3 N_c^2 \int d^5x \sqrt{-g} \left[R - \frac{4}{3} \frac{(\partial\lambda)^2}{\lambda^2} + V(\lambda) - \frac{Z(\lambda)}{2N_c^2} (\partial\alpha)^2 \right], \qquad (10)$$

  where $M_p^3 = 1/(16\pi G_5 N_c^2)$.

- $\lambda = e^{\phi}$ is the holographic 't Hooft coupling with potential $V(\lambda)$.
- $\alpha(r)$ is the holographic θ angle.
- $Z(\lambda)$ encodes the interaction of the dilaton with the axion and it comes from α' corrections.
- Requiring IHQCD free energy to follow Stefan-Boltzmann law for a gluon gas at high T, we fix $(M_p \ell)^{-3} = 45\pi^2$.

IHQCD

The vacuum

- The zero temperature vacuum solution is of the type

$$ds^2 = e^{2A_0(r)}(dr^2 + \eta_{\mu\nu}dx^\mu dx^\nu)\ , \quad \lambda = \lambda(r)\,, \qquad (11)$$

  where $e^{A_0(r)}$ is the metric scale factor corresponding to the energy scale of QCD.

- As $r \to 0$ (boundary of spacetime),

$$e^{A_0(r)} \to \frac{\ell}{r} + \mathcal{O}\left(\frac{1}{\log(r)}\right)\ , \quad \lambda \to -\frac{1}{\log r}\,, \qquad (12)$$

  so as to match the running of the large-N_c YM coupling.

- The axion field contribution to the vacuum energy is of order $\mathcal{O}\left(1/N_c^2\right)$.

IHQCD

Finite Temperature

- IHQCD action has black hole solutions which they describe finite temperature QCD

$$ds^2 = e^{2A(r)}\left(\frac{dr^2}{f(r)} - f(r)dt^2 + dx^i dx_i\right) \tag{13}$$

- Two branches of black hole solutions exist,

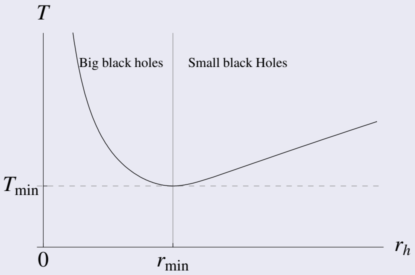

- The large black holes are the thermodynamically preferred solutions. A first order confinement/deconfinement phase transition happens.

IHQCD

The dilaton potential

- The running of 't Hooft coupling in YM fixes the UV asymptotics of $V(\lambda)$

$$V(\lambda) \simeq \frac{12}{\ell^2}\left(1 + v_0\lambda + v_1\lambda^2 + \mathcal{O}(\lambda^3)\right). \tag{14}$$

- The criteria for confinement and asymptotic linear Regge trajectories of the glueball spectra fix the IR behavior of $V(\lambda)$

$$V(\lambda) \propto \lambda^{\frac{4}{3}}\sqrt{\log\lambda}\,. \tag{15}$$

The action

- The axion part of the action in IHQCD is reminded

$$S_\alpha = -\frac{1}{2}M_p^3 \int d^5x\sqrt{-g}\, Z(\lambda)(\partial\alpha)^2\,. \tag{16}$$

- $\alpha(x,r)$ is dual to $q(x)$. $\alpha(r=0)=\kappa\,\theta$, where κ is a constant and θ is the YM θ-angle.
- The asymptotics of $Z(\lambda)$ are

$$Z(\lambda) \propto \begin{cases} Z_0 + \mathcal{O}(\lambda), & \lambda \to 0, \\ \lambda^4 + \mathcal{O}(1/\lambda), & \lambda \to \infty, \end{cases} . \tag{17}$$

It's IR asymptotics is decided by requiring universal linear glueball Regge trajectories for large excitation number.

The axion background

- The axion equation of motion in a background of the from, (11), is

$$\partial_r \left(Z(\lambda(r))\, e^{3A_0}\, \partial_r \alpha(r) \right) = 0\,. \tag{18}$$

- The solution reads

$$\alpha(r) = \theta + 2\pi k + C \int_0^r \frac{dr}{\ell} \frac{1}{e^{3A_0} Z(\lambda)} \quad , \quad k \in \mathbb{Z}\,. \tag{19}$$

- The on-shell action is the vacuum energy per volume

$$\mathcal{E}(\theta) = -\frac{M_p^3}{2\ell} C\, \alpha(r) \Big|_{r=0}^{r=\infty}\,. \tag{20}$$

Requiring to have contribution only from the UV boundary we find $C = \langle q(x) \rangle = (\theta + 2k\pi) \left(\int_0^\infty \frac{dr}{\ell} \frac{1}{e^{3A_0} Z(\lambda)} \right)^{-1}$.

- Hence, the vacuum energy reads

$$\mathcal{E}(\theta) = \frac{M_p^3}{2} \frac{(\theta + 2k\pi)^2}{\int_0^\infty dr \frac{1}{e^{3A_0} Z(\lambda)}} . \tag{21}$$

- and the topological susceptibility is

$$\chi \equiv \frac{d^2\mathcal{E}(\theta)}{d\theta^2} = \frac{M_p^3}{\int_0^\infty \frac{dr}{e^{3A_0(r)} Z(\lambda(r))}} . \tag{22}$$

The interaction with dilaton ($Z(\lambda)$)

- The simplest form for $Z(\lambda)$, which was first considered in IHQCD, is

$$Z(\lambda) = Z_0(1 + c_4\lambda^4)\,, \tag{23}$$

- Z_0 is fixed by matching to the large-N YM lattice results for the topological susceptibility,

$$\chi \simeq (191\text{MeV})^4 \Rightarrow \kappa^2 Z_0 = 33.25 \tag{24}$$

(Vicari-Panagopoulos)

The interaction with dilaton ($Z(\lambda)$)

- c_4 is fixed by matching to lattice results for the first axial glueball mass.

$$m_{0^{-+}}/m_{0^{++}} = 1.50 \Rightarrow c_4 = 0.26\,. \tag{25}$$

- The next mass of the 0^{-+} tower is very well predicted

$$(m_{0^{*-+}}/m_{0^{++}})_{IHQCD} = 2.10\ ,\ (m_{0^{*-+}}/m_{0^{++}})_{lat.} = 2.11(6)\,. \tag{26}$$

(Morningstar-Peardon)

The fluctuation equation

- The linear fluctuation equation of the axion is considered in the black hole background,

$$\frac{1}{Z(\lambda(r))\sqrt{-g}}\,\partial_r\left[Z(\lambda(r))\sqrt{-g}\,g^{rr}\partial_r\delta\alpha(r,k^\mu)\right]-g^{\mu\nu}k_\mu k_\nu\,\delta\alpha(r,k^\mu)=0\,, \tag{27}$$

where we have considered solutions of the form

$$\delta\alpha(r,x^\mu)=\int\frac{d^4k}{(2\pi)^4}\,e^{ikx}\,\delta\alpha(r,k^\mu)\,a(k^\mu)\,. \tag{28}$$

The UV normalization is $\lim_{r\to 0}\delta\alpha(r,k^\mu)=1$, and infalling wave boundary condition is set on the horizon.

- The on shell action of the fluctuation is

$$S_\alpha^{\text{on-shell}}=\int\frac{d^4k}{(2\pi)^4}\,a(-k^\mu)\,\mathcal{F}(r,k^\mu)\,a(k^\mu)\Big|_0^{r_h}\,,$$
$$\mathcal{F}(r,k^\mu)\equiv-\frac{M_p^3}{2}\,\delta\alpha(r,-k^\mu)\,Z(\lambda(r))\,\sqrt{-g}\,g^{rr}\,\partial_r\delta\alpha(r,k^\mu)\,. \tag{29}$$

Γ_{CS}

AdS/CFT yields that the retarded Green's function is

$$\hat{G}_R(\omega, \vec{k}) = -2 \lim_{r \to 0} \mathcal{F}(r, k^\mu). \tag{30}$$

Solving the fluctuation equation for $\omega = 0$ and $\vec{k} = 0$ we find

$$\delta\alpha = C_1 + C_2 \int_0^r \frac{dr'}{Z(\lambda(r'))e^{3A(r')}f(r')}, \tag{31}$$

UV normalization fixes $C_1 = 1$. For non-zero but small ω, we expect $C_2 \propto \omega$. Expanding (31) close to the horizon we have

$$\delta\alpha = 1 + \frac{C_2}{Z(\lambda_h)\, e^{3A(r_h)}\, f'(r_h)} \log(r_h - r) + \mathcal{O}(r_h - r)\,. \tag{32}$$

Γ_{CS}

Then, we find

$$\lim_{r\to 0} \mathcal{F}(r,k^\mu) = -\frac{M_p^3}{2}\, C_1\, C_2.\ (\omega << T, \vec{k}=0)\,. \tag{33}$$

Going back and solving the fluctuation equation at $r \to r_h$ for finite ω and setting the outgoing solution to zero, we have

$$\delta\alpha = C_+(r_h-r)^{\frac{i\omega}{4\pi T}} + C_-(r_h-r)^{-\frac{i\omega}{4\pi T}} = C_- - i\frac{\omega}{4\pi T}\, C_-\, \log(r_h-r) + \mathcal{O}(\omega^2/T^2)\,. \tag{34}$$

Matching the two solutions, we find that in the limit $\omega \to 0$, $C_- = 1$ and $C_2 = -i\omega\, Z(\lambda_h)\, e^{3A(r_h)}$. We finally have

$$\frac{\Gamma_{CS}}{sT/N_c^2} = \frac{\kappa^2 Z(\lambda_h)}{2\pi}\,, \tag{35}$$

which implicitly depends on T, through $Z(\lambda_h)$

Holographic Γ_{CS}

- On the large black hole branch, $\Gamma_{CS}/(sT/N_c^2)$ is bounded from below by its value in the $T\to\infty$ limit, $\lim_{T\to\infty}\frac{\Gamma_{CS}}{sT/N_c^2}=\frac{\kappa^2 Z_0}{2\pi}$.

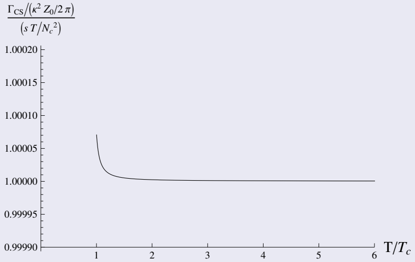

Figure : The numerical result for $\Gamma_{CS}/(sT/N_c^2)$ in terms of T/T_c for the simplest $Z(\lambda)$, (23). $\Gamma_{CS}/(sT/N_c^2)$ is approximately constant except for the region close to T_c where it slightly increases.

- Due to the small values of λ_h in the large black hole branch, terms with lower power than λ^4 in $Z(\lambda)$ play an important role in Γ_{CS}.

Different parameterization of $Z(\lambda)$

- The largest polynomial correction to $Z(\lambda)$ for small values of λ is linear,

$$Z(\lambda) = Z_0 \left(1 + c_1\lambda + c_4\lambda^4\right) . \tag{36}$$

  Upon fitting to the first axial glueball mass we find that for any $c_1 > 0$ there is a c_4 for which the value of the second excited state exhibits at most 3% discrepancy from the large N_c lattice value.
- Simple non-monotonic $Z(\lambda)$s with the desired asymptotics, (17), produce glueball masses that deviate from lattice results more than 10%.
- The assumption that $Z(\lambda)$ is monotonic in λ sets the bound $Z(\lambda) > Z_0$ for any temperature T.

Different parameterization of $Z(\lambda)$

Figure : IHQCD masses of the 0^{-+} glueball states with excitation number n, normalized to the 0^{++} mass for various (c_1, c_4). From the top (red) dots to the bottom (blue) dots the values of (c_1, c_4) increase, $(c_1, c_4) = (0, 0.26), (0.5, 0.87), (1, 2.2), (5, 24), (10, 75), (20, 230), (40, 600)$. The two horizontal blue lines with surrounding blue bands indicate the results and errors, respectively, of the large-N_c YM lattice masses of the lowest and first excited states, $n = 1$ and $n = 2$, (Morningstar-Peardon).

Γ_{CS}

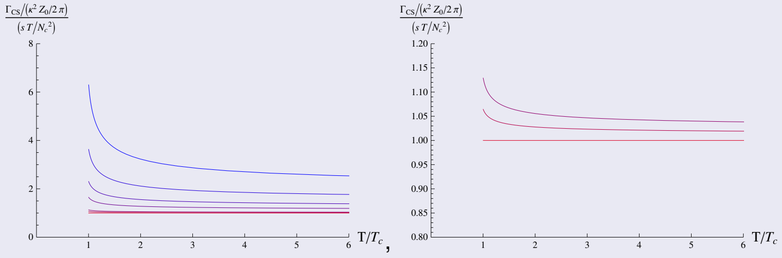

Figure : (a) The numerical result for $(\Gamma_{CS}/\kappa^2 Z_0/2\pi)/(sT/N_c^2)$, as functions of T/T_c, for the $Z(\lambda)$ in eq. (36), for increasing values of the parameters (c_1, c_4), from the bottom (red) curve to the top (blue) curve, $(c_1, c_4) = (0, 0.26), (0.5, 0.87), (1, 2.2), (5, 24), (10, 75), (20, 230), (40, 600)$. (b) Close-up of the curves for (from bottom to top) $(c_1, c_4) = (0, 0.26), (0.5, 0.87), (1, 2.2)$. In all of these cases, as T approaches T_c from above $\Gamma_{CS}/(sT/N_c^2)$ increases by anywhere from 0.01% up to a factor greater than six. The increase occurs mostly between $2T_c$ and T_c.

Γ_{CS}

- A numerical estimate of Γ_{CS} near the confinement-deconfinement phase transition is

$$\Gamma_{CS}(T_c)/T_c^4 = 0.31 \times \frac{\kappa^2 Z(\lambda_c)}{2\pi} > 0.31 \times \frac{\kappa^2 Z_0}{2\pi} = 1.64\,, \qquad (37)$$

where we have used the lattice result for the entropy density, $s(T_c) = 0.31 N_c^2 T_c^3$, (Lucini-Teper-Wenger).

- An upper bound can also be set to $\Gamma_{CS}(T_c)$ by considering a $Z(\lambda)$ of the form of (36), with $c_1 = 5$ and $c_4 = 50$, which produce the axial glueball spectrum within one sigma with respect to the lattice results. Then,

$$1.64 \le \Gamma_{CS}(T_c)/T_c^4 \le 2.8\,. \qquad (38)$$

Γ_{CS} in $\mathcal{N}=4$ sYM.

- The result in large-N_c strongly coupled $\mathcal{N}=4$ sYM is

$$\Gamma_{\rm CS}^{\mathcal{N}=4} = \frac{\lambda_t^2}{2^8\pi^3}\, T^4\,. \qquad (39)$$

(Son-Starinets).

- For some typical values $\lambda_t = 6\pi$ and $N=3$ we have

$$\Gamma_{\rm CS}^{\mathcal{N}=4}/T^4 \simeq 0.045\,, \qquad (40)$$

which much smaller than the IHQCD result.

- A naive extrapolation of the perturbative result, which is valid for $\alpha_s << 1$, $(-\ln\alpha_s)^{-1} << 1$, to $\alpha_s = 0.5$,

$$\Gamma_{CS}^{(per.)}(T_c)/T_c^4 = 30\alpha_s^5 \simeq 1 \qquad (41)$$

(Moore-Tassler)

$\mathrm{Im}\, G_R(\omega, \vec{k} = 0)$

- We now calculate the axion spectral function ($\mathrm{Im} G_R(\omega, \vec{k})$)for non-zero ω and $|\vec{k}|$. We firstly calculate it for $\vec{k} = 0$.
- For small ω, the axion fluctuation equation yields $\mathrm{Im}\, G_R(\omega, \vec{k} = 0) \propto \omega$.
- For large ω, we expect $\mathrm{Im}\, G_R(\omega, \vec{k} = 0) \propto \omega^4$ because the theory is conformally invariant in the UV and $q(x^\mu)$ is dimension four.

Im $G_R(\omega, \vec{k} = 0)$

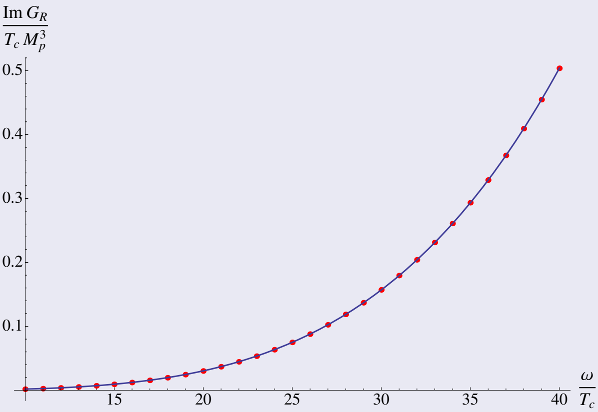

Figure : Im $G_R(\omega, \vec{k} = 0)/(T_c M_p^3)$ as a function of ω/T_c, at T_c, for the $Z(\lambda)$ in eq. (23). The red dots are our numerical results that match the solid blue curve, $(1.6 \times 10^{-7}) \times (\omega/T_c)^{4.051}$, which is the expected large ω behavior of the spectral function.

The renormalized $\mathrm{Im}\, G_R(\omega, \vec{k}=0)$

- The ω^4 scaling of $\mathrm{Im}\, G_R(\omega, \vec{k}=0)$ at large ω is a divergence in the coincidence limit of the two-point function, which may overwhelm peaks in $\mathrm{Im}\, G_R(\omega, \vec{k})$, rendering them practically invisible.
- To eliminate the large-ω divergence we compute $G_R(\omega, \vec{k})$ at two different temperatures, T_1 and T_2, and then take the difference,

$$\Delta G_R(\omega, \vec{k}; T_1, T_2) \equiv G_R(\omega, \vec{k})\Big|_{T_2} - G_R(\omega, \vec{k})\Big|_{T_1} . \tag{42}$$

The renormalized $\mathrm{Im}\, G_R(\omega, \vec{k} = 0)$

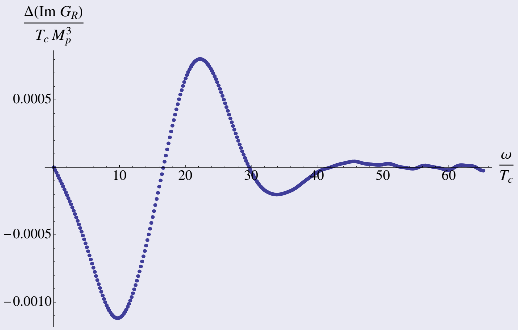

Figure : The difference $\Delta\mathrm{Im}\, G_R(\omega, \vec{k} = 0; T_c, 2T_c)/(T_c M_p^3)$ as a function of ω/T_c, for the $Z(\lambda)$ in eq. (23). The difference goes to zero as $\omega/T_c \to \infty$. The prominent minimum at $\omega/T_c \approx 10$ and maximum at $\omega/T_c \approx 22$ indicate a shift in spectral weight with increasing T, possibly from the motion of a peak in the spectral function. There is a peak at $\omega \simeq 20T_c \simeq 1600$MeV and width $\sim 10T_c \sim 1300$MeV.

The renormalized $\mathrm{Im}\, G_R(\omega, \vec{k})$

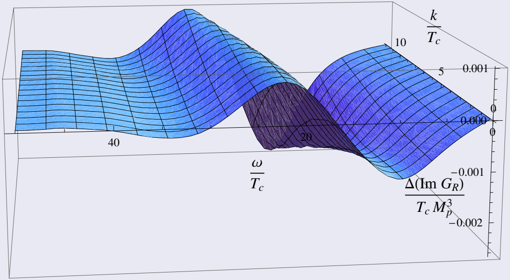

Figure : $\Delta \mathrm{Im}\, G_R(\omega, \vec{k} = 0; T_c, 2T_c)/(T_c M_p^3)$ in terms of ω/T_c and $|\vec{k}|/T_c$, for the $Z(\lambda)$ in eq. (23). As $|\vec{k}|$ increases up to $|\vec{k}|/T_c \approx 10$, the largest peak shifts from $\omega/T_c \approx 22$ up to $\omega/T_c \approx 30$. The width of the peak changes very little.

Conclusions

- The Chern-Simons diffusion rate was calculated in IHQCD for $T > T_c$ and found it proportional to $Z(\lambda_h)$, which is the value of the axion-dilaton potential, at $\lambda = \lambda_h$. λ_h is the value of the dilaton at the black hole horizon.
- Assuming that $Z(\lambda)$ is a monotonic function of λ, we argued that it is bounded from below by it's value at $T \to \infty$.
- This is argued to be true for a general class of (3+1)-dimensional, confining, strongly-coupled, large-N_c theories with holographic duals.
- A large value of $\Gamma_{\rm CS}(T_c)/T_c^4$, compared to the $\mathcal{N} = 4$ sYM and the extrapolated pertrubative results, is favored in IHQCD.
- The presence of a long lived excitation of mass of order of the lightest 0^{-+} glueball at $T = 0$ was found by studying the axion spectral function.

Future directions

- Fixing $Z(\lambda)$ by the fitting to a lattice calculation of the Euclidean 2-point function of $q(x^\mu)$ is an important future plan.
- Calculate Γ_{CS} in the presence of a background magnetic field.
- Calculate $\Gamma_{\rm CS}$ in a model which incorporates the flavor degrees of freedom as well (V-QCD). Then, the axion is coupled to the axial vector flavor current and the pseudoscalar phase of the tachyon. Hence, $\Gamma_{\rm CS}$ is expected to be affected by tachyon dynamics.

Thank you

The axion profile

- Typical behavior of the axion in a confining background solution ($T \leq T_c$) with IR normalizable boundary conditions. The axion is interpreted as the running θ-angle of the dual field theory.

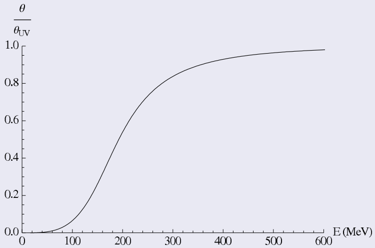

- In the deconfined background ($T > Tc$), the only non-singular solution is $\alpha(r) = \theta =$ const. and the topological susceptibility is zero.

Γ_{CS}

- In equilibrium states with finite temperature, Γ_{CS} is given by

$$\Gamma_{CS} = -\lim_{\omega\to 0} \frac{2T}{\omega} \operatorname{Im} G_R(\omega, \vec{k}=0)\,, \tag{43}$$

  where $G_R(\omega, \vec{k})$ is the Fourier tranformation of the retarted Green function of $q(x^\mu)$.
- Γ_{CS} can be related to ΔN_5 by a fluctuation-dissipation relation of the form

$$\frac{d\Delta N_5}{dt} = -\Delta N_5 \frac{6N_f}{N_c}\frac{\Gamma_{\text{CS}}}{T^4}\,. \tag{44}$$

- Hence non-vanishing ΔN_5 induces topological fluctuations which balance ΔN_5 and relax it back to zero.